Ultra Sensitive Quantification of Hg^{2+} sorption by Functionalized Nanoparticles using Radioactive Tracker Spectroscopy

Carlos O. Amorim,[*a] João N. Gonçalves,[a] Daniela S. Tavares,[b,c] Abel S. Fenta,[a,d,e]
Cláudia B. Lopes,[c,f] Eduarda Pereira,[b] Tito Trindade,[c] João G. Correia,[e,g]
Vítor S. Amaral[a]

[a] *Physics Department and CICECO, University of Aveiro, 3810-193 Aveiro, Portugal; E-mail:amorim5@ua.pt*
[b] *Department of Chemistry and CESAM, University of Aveiro, 3810-193 Aveiro, Portugal*
[c] *Department of Chemistry and CICECO, University of Aveiro, 3810-193 Aveiro, Portugal*
[d] *KU Leuven, Instituut voor Kern- en Stralingsfysica, 3001 Leuven, Belgium*
[e] *CERN, EP Division, 1211 Geneva 23, Switzerland*
[f] *CIIMAR, Interdisciplinary CTR of Marine and Environmental, 4050-122 Porto, Portugal*
[g] *C2TN, Instituto Superior Técnico, University of Lisbon, 2686-953 Sacavém, Portugal*
E-mail:amorim5@ua.pt

January 22, 2018

Abstract

We present an ultra sensitive method to quantify the uptake of Hg by dithiocarbamate functionalized magnetic nanoparticles using radioactive tracker spectroscopy. We show a lower limit of detection of about 10fg L^{-1}, much lower than any other known techniques used to determine the uptake of Hg (about 10^4 more sensitive), without the need of digesting or processing the sorption agent. Such high sensitivity enables the characterization of Functionalized Nanoparticles as Hg sorbents in natural waters, where the low Hg concentration is very difficult to detect using current analytical methods such as absorption/fluorometry methods (namely Cold Vapour Atomic Absorption/fluorescence Spectroscopy).

Radioactive Trackers also give the ability to track the sorbed element, allowing the reconstruction of the path made by the sorbed element during the uptake process, unveiling further information about the impact of toxic metals in the environment and living beings.

1 Introduction

The rapid development and expansion of industry have increased the contamination levels of toxic metal ions in aquatic systems. Even at low concentration, such metals present a significant risk to biota and humans, given their persistence, toxicity and bioaccumulation and bio magnification along the food chain. Examples of metal contaminants include mercury (Hg), lead (Pb), cadmium (Cd), copper (Cu), nickel (Ni), and zinc (Zn). Mercury, in particular, is considered one of the most hazardous contaminants due to its toxicological and biogeochemical behaviour, causing many severe adverse health effects on the nervous, digestive and immune systems, lungs, kidneys, skin and eyes.

In order to remove or reduce the level of metals in effluents and waters, the scientific community has investigated effective solutions. Ion exchange, membrane separation, chemical precipitation, filtration and sorption are generally investigated methods[1].

Sorption is a common method in practical use due to its ease of operation and the availability of a wide range of sorbents[2,3]. Preparation and application of nanomaterials as sorbents for the removal of metals from waters has increased rapidly in recent years. Nanosorbents have several advantages such as large specific surface area (when comparing to their bulk equivalent), enhanced active sites and the ability to be functionalized with different chemical groups which can enhance their sorption efficiency[4,5].

Iron oxide nanoparticles (NP), in particular, form a promising class of magnetic sorbents for environmental applications, due to their separation capability from aqueous solutions by application of an external magnetic field[6,7]. In recent work, we developed magnetic sorbents based on silica-coated magnetite NP functionalized with dithiocarbamate (DTC) groups for the uptake of Hg(II) from water. Results showed that the magnetic sorbents are highly efficient at removing mercury from contaminated waters, by decreasing the metal concentration to values lower than the guideline values for drinking water ($1\mu g\ L^{-1}$)[8,9].

Despite the work already done to characterize Hg sorption by Functionalized Nanoparticles (FNP), the methods utilized to perform that characterization possess several limitations, namely the lower limit of detection, calibration problems and the fact that the sorption percentage is always measured indirectly (usually sorption studies are made by mass balance, i.e. the amount of Hg sorbed is estimated by measuring the amount of Hg in the water and not the amount sorbed by the NP) increasing the difficulty of studying the behaviour of the NP when subjected to external factors (like changes in temperature).

In this work we present an alternative method for determining the uptake of toxic metal ions using radioactive isotopes, demonstrated here with the specific case of Hg. This approach enables direct measurements of the element uptake, has tracking capabilities and shows a much lower limit of detection (10fg L^{-1}) when compared to typical methods of measurement (0.1ng L^{-1} for Cold Vapour Atomic Fluorescence (CVAFS)).

This low limit of detection enables the characterization of FNP as Hg sorbents for very low Hg concentration waters allowing to tailor and certify Hg concentrators. These concentrators can be used to purify waters that, despite having legal concentrations of Hg, could pose a long term environmental threat due to Hg's bioaccumulation and biomagnification properties, mainly in higher trophic levels.

2 Experimental Details

Two types of sorbent materials were used in this work: silica coated magnetite iron oxide particles - Fe_3O_4, and silica coated magnetite iron oxide particles functionalized with DTC groups.

The synthesis of NP includes two distinct steps according with the procedure described by Tavares et al[8]. Firstly, the synthesis of the magnetic core (cubic (A-Fe_3O_4) and nearly spherical (B-Fe_3O_4) NP) by oxidative hydrolysis of $FeSO_4.7H_2O$ under alkaline conditions, as described in previous work by Oliveira et al.[10] and Girginova et al[11]. Then its encapsulation and functionalization with DTC groups via alkaline hydrolysis of TEOS in the presence of a siloxydithiocarbamate precursor siloxydithiocarbamate, as described by Tavares et al[8].

We studied 6 types of nanoparticles. The A_2 (B_2) NP which are cubes (spheres) made of a magnetite core coated with silica with a total side (diameter) of $\approx$ 100 nm (50nm). We also studied FNP A_{4-} (B_{4-}) and FNP A_{4+} (B_{4+}) which are actually just the A_2 (B_2) NP functionalized with the DTC functional group with different amount of TEOS (the - or + subscripts represent less and more functionalization respectively). A schematic representation can be seen in figure 1.

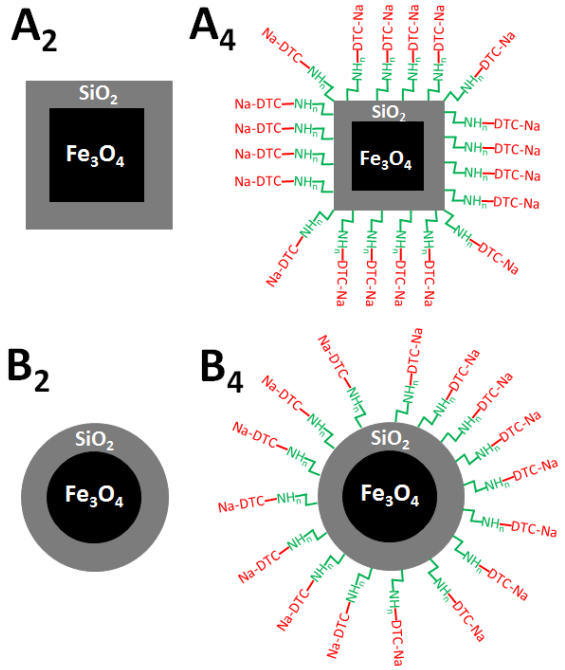

Figure 1 Schematic representation of A_2, B_2, A_4 and B_4 Nanoparticles. These representations are not to scale.

A systematic study was made using 6 sets of 3 measurements (adding up to a total of 18 measurements). Each set of measurements consisted of 3 test tubes ($\varnothing \approx 8$ mm) containing (550 ± 50) μg of a given type of NP (each set of measurements had a different type of NP)[1]. The inside walls of every test tube were previously saturated with Hg ions using a 1g L^{-1} aqueous solution of $Hg(NO_3)_2$ and then dried.

The ^{199m}Hg ion beam was produced online at ISOLDE by the bombardment of a UCx target with the 1.4 GeV proton beam from the CERN Proton Synchrotron Booster and selective Hg ionization using the RILIS (Resonance Ionization Laser Ion Source)[12,13]. The target/ion source parameters were optimized to enhance the ratio[2] r between ^{199m}Hg and ^{199}Hg (in our case about 50%).

The Hg beam with 30 keV energy was then redirected to the GLM beam line where a sample holder was mounted inside a biophysics chamber under vacuum (10^{-5} mbar). The implantation was done in 0.2 mL of a frozen (solid) solution of 100g of KNO_3 per liter of de-ionized (DI) water sustained inside a Teflon cup. The Teflon cup fits a copper holder that is connected to a cold finger immerged into a liquid nitrogen bath, to ensure that the ice does not melt/sublimate under vacuum.

The experimental Hg sorption characterization procedure is summarized by the scheme of figure 2 and presented with detail in the text written below.

The nanoparticles were dispersed in 1 mL of DI-water for some minutes (resorting to a ultrasound homogenizer) before adding the radioactive water to avoid agglomeration of the magnetic NP. Finally, after melting the radioactive ice, the former was added to the test tube with the FNP in suspension.

The activity of the resulting solution was measured using a high purity germanium gamma spectrometer (ORTEC GWL-120-15 Coaxial HPGe Detector). Then, using the ultrasound homogenizer, the solution containing both the FNP and the radioactive Hg was sonicated during 20 minutes (to increase the interaction between the Hg ions and the NP). After homogenization the activity of the solution was once again measured (as a control measurement).

To determine the amount of Hg sorbed by the different NP, all the liquid in the test tube was removed (using a magnet to separate the magnetic NP from the liquid portion). The activity of the NP alone was measured in the Ge detector to infer the quantity of ^{199m}Hg coordinated to the NP themselves (figure 3) and then compared with the activity of the solution containing both the radioactive water and the NP in suspension.

A reference sample was prepared in the conditions mentioned above, but using the FNP dispersed in non radioactive DI-water. As it can be seen in the inset of figure 3 only electronic noise was detected (always lower than 6 counts) when we measured both this reference sample and the empty detector sample holder for 5 minutes.

3 Results and Discussion

The total number of Hg (N_{Hg}) ions implanted in the frozen DI-water can be determined using equation 1:

$$N_{Hg} = \int_0^{t_i} i(t)dt \approx It_i \,, \tag{1}$$

where $i(t)$ is the implanted Hg ions current as a function of time, which can be written as $i(t) \approx I$ since it is approximately constant through all the implantation time.

Using equation 2:

$$\begin{aligned} N_i &= N_{Hg} \cdot re^{-\lambda t_i} = rIt_i e^{-\lambda t_i} \\ &\leftrightarrow N_{Hg} = \frac{N_i}{re^{-\lambda t_i}} \,, \end{aligned} \tag{2}$$

we can relate N_{Hg} with the measurable N_i, where N_i is the number of radioactive ^{199m}Hg implanted in ice, $\lambda = {}^{ln(2)}/_{\tau_{1/2}}$ ($\tau_{1/2} = 2559.6s$ is the half-life time of ^{199m}Hg), and t_i is the implantation time.

To measure N_i using the HPGe detector, we should first relate N_i with the integral Γ as we can see in equation 3:

[1] For example for the A_2 NP set, each test tube was labelled as A_{2a}, A_{2b} and A_{2c}.

[2] which is $r = \frac{N_i}{N_{Hg}} = \frac{^{199m}\text{Hg}}{(^{199}\text{Hg} + ^{199m}\text{Hg})}$

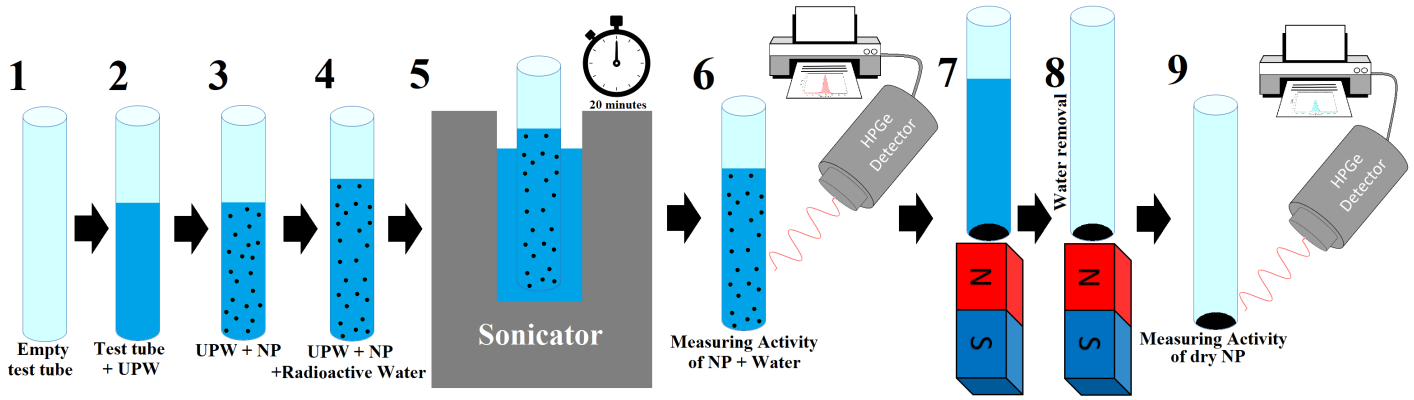

Figure 2 Schematic representation of the experimental procedure done to characterize the Hg sorption efficiency by the NP.

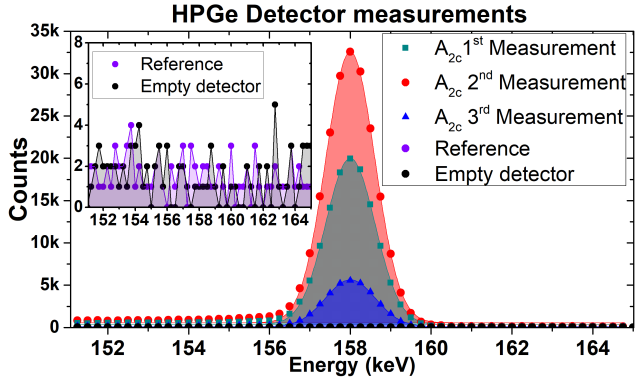

Figure 3 Spectral distribution for 3 different measurements of the same sample, a reference sample comprised of sample dispersed in non radioactive DI-water and a measurement with an empty detector sample holder. The HPGe allows an energy specific analysis.

$$\Gamma = \int_{t_1}^{t_2} \frac{dN_i}{dt} dt = \int_{t_1}^{t_2} \lambda N_i e^{-\lambda t} dt \leftrightarrow$$
$$\leftrightarrow N_i = \frac{\Gamma}{\left(e^{-\lambda t_1} - e^{-\lambda t_2}\right)} , \tag{3}$$

where t_1 and t_2 are the times when the measurement of the sample began and ended respectively[14–16]. This integral (Γ) is related to the spectral distribution of a ^{199m}Hg characteristic gamma emission peak (we used the 158.38 keV peak which corresponds to $\eta \approx$ 52.3% of ^{199m}Hg decays), as we can observe in figure 3 and in equation 4.

$$\Gamma = \frac{A}{\eta \cdot k \cdot \theta \cdot b} . \tag{4}$$

Finally, N_i is given by equation 5:

$$N_i = \frac{A}{\left(e^{-\lambda t_1} - e^{-\lambda t_2}\right)} \cdot \frac{1}{\eta \cdot k \cdot \theta \cdot b} , \tag{5}$$

where k is the live time of the HPGe detector, b is the energy binning, A is the spectral area of the 158.38 keV peak and θ is a solid angle correction factor (which is calculated taking into account the detector efficiency for 158.38 keV, its area and its distance from the sample). The error associated with the indirect measurement of N_i (ΔN_i) is shown in equation 6:

$$\Delta N_{Hg} \approx \Delta N_i =$$
$$= \left| \frac{1}{\eta \cdot \left(e^{-\lambda t_1} - e^{-\lambda t_2}\right)} \right| \cdot \left[\left| \frac{\Delta A}{k \cdot \theta \cdot b} \right| + \right.$$
$$\left. + \left| \frac{A \cdot \Delta\theta}{k \cdot \theta^2 \cdot b} \right| + \left| \frac{A \cdot \Delta k}{k^2 \cdot \theta \cdot b} \right| \right] , \tag{6}$$

where ΔA is the area fit error (which always surpasses the uncertainty due to the radioactive decay). All uncertainties are determined at maximum values to unsure that the final error determination is always the upper bound.

Sorption results of all the FNP are shown in table S1 for a typical integration time $t_2 - t_1$ of the order of 1-5 minutes.

Observing table S1 we can infer that we have concentrations of Hg as low as 4 ng L^{-1} (in the order of the lower limit of detection of typical fluorometry analysis). Actually the sorption values seem to be independent of the concentration of Hg for this concentration regime (if there is any relation to the concentration its behaviour falls inside the error margin).

We infer the sorption value for each type of NP as an average of all the sorption values of its correspondent type of NP, as we can see in the last 2 columns of table S1 and in figure 4.

It is clear in figure 4 that NP functionalized with DTC (A_4 and B_4) present much higher Hg uptake than the silica coated magnetite NP (A_2 and B_2).

The obtained results agree very well with results obtained from CVAFS measurements made previously. In figures 5, 6 and 7 it is clear that the results obtained using radioactive trackers follow pretty well the sorption tendency reported in Tavares et al[8,9] using CVAFS. Some deviations from the these results can arise from the fact that we used sonication for all the 20 minutes instead of mechanical stirring, which can slightly change the kinetics of the reaction.

The higher sorption efficiency of B_2 when compared with A_2 is observable in both methods of measurement in figure 5.

The higher uptake of the functionalized A_{4-} when compared with B_{4-} is also visible in figure 6 either for the radioactive trackers as in CVAFS measurements.

Finally, in the NP with more functionalization A_{4+} and B_{4+}, the sorption rates in the beginning of the reaction are so high that we cannot distinguish uptake efficiencies between these two FNP using only one point, despite being compatible with both kinetic behaviours obtained from CVAFS (figure 7).

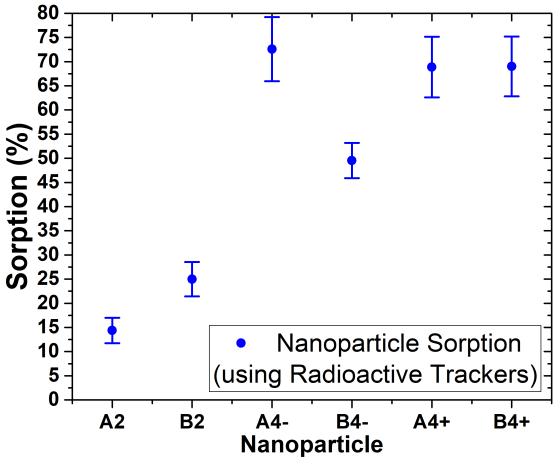

Figure 4 Hg uptake summary for all types of Nanoparticles studied using radioactive trackers as characterization method.

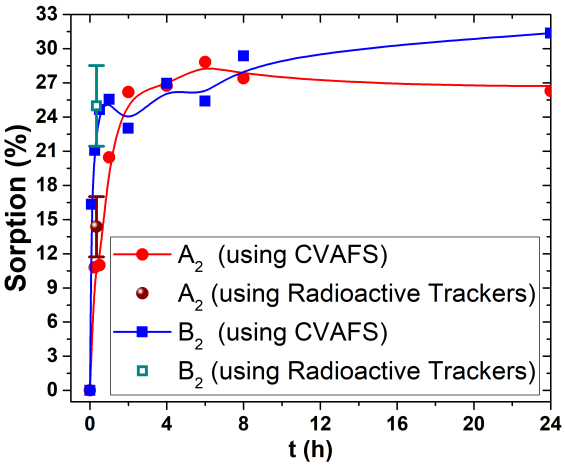

Figure 5 Comparison between the sorption efficiency of A_2 and B_2 NP measured using CVAFS[8,9] and radioactive trackers.

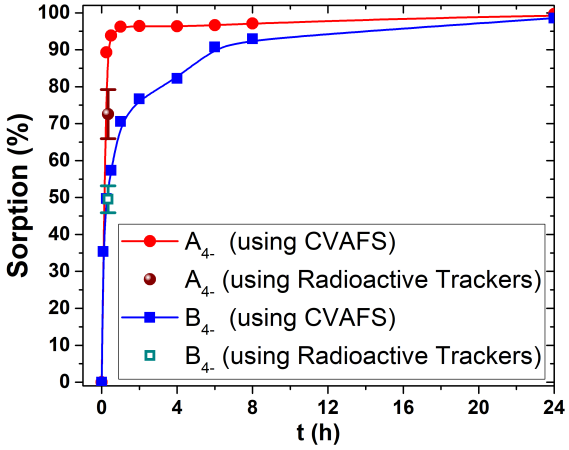

Figure 6 Comparison between the sorption efficiency of A_{4-} and B_{4-} NP measured using CVAFS[8,9] and radioactive trackers.

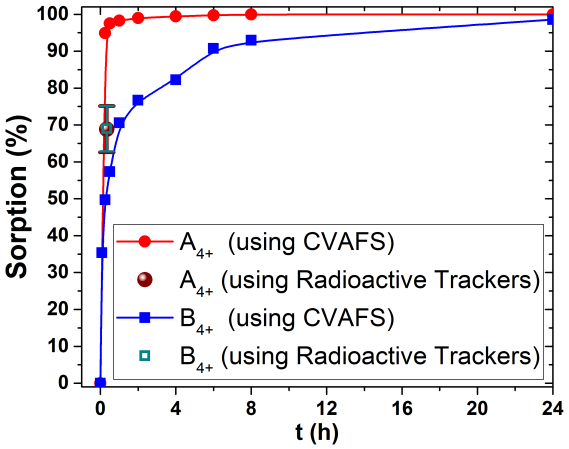

Figure 7 Comparison between the sorption efficiency of A_{4+} and B_{4+} NP measured using CVAFS[8,9] and radioactive trackers.

4 Advantages of Radio-Trackers for Hg uptake characterization

The utilization of radioactive isotopes to infer the uptake of a given element is already well known in the literature namely for Hg sorbents, nonetheless its usage does not make the most of radioactive trackers capabilities[17–21]. As a matter of fact, aspects such as the sensitivity, traceability and element specificity are not exploited in reported uptake studies using radioisotopes, where a more qualitative approach is favoured, underusing the radioisotopes characteristics[17–21].

This manuscript works as a proof of concept for the usage of radioactive trackers as a means of a very sensitive quantitative analysis of toxic metals uptake studies (Hg in particular). We also highlight here that this approach shows several advantages when compared with typical methods of analysis.

4.1 High sensitivity

Current fluorescence spectroscopy shows lower limits of detection in the order of the ng L^{-1}, however these values depend heavily in the chemical environments of the fluorophore, amount of impurities as well as the amount of processing/digestion needed[22–24]. The typical lower limit of detection for Hg is in the order of the tens of ng L^{-1} [22].

In this work we report values as low as 4 ng L^{-1}, however this value is far from the lower limit of detection of this experimental *setup*. In fact, the activity of our samples was so high (even for this low amount of Hg) that we measured the samples far from the detector (about 12.8 cm). Such distance was corrected in the solid angle factor present in equation 4 (being the higher source of experimental error). By placing the samples near the detector we would be able to detect concentrations of Hg in the order of pg L^{-1}.

Furthermore the detector container allows a sample volume of 120 mL (100 times higher that the quantity used in this manuscript). Once we detect the total amount of γ photons emitted from the sample, this would place the lower limit of detection for this particular isotope (^{199m}Hg) in this simple *setup* at least in the order of **10fg L^{-1}**.

4.2 Direct Measurement

In order to monitor the Hg uptake by nanosorbents, the concentration of Hg in treated water is usually assessed and plotted as a function of contact time. This is an indirect measurement, since it does not tell us the amount of Hg sorbed by the NP but only the amount present in the water.

Since we measure the activity directly in the dry NP we can be

sure that the mercury is sorbed by the nanoparticles themselves and not elsewhere. This peculiarity allows us to make studies directly in the NP, like the uptake stability with the temperature (will the Hg ions remain sorbed by the NP even if we increase their temperature? If not, at which temperature?).

Since this approach relies on the emission of γ photons (which are mostly transparent to most mediums/matrices), we are able to determine the uptake of a given sample independently of the fact of it being in a solid, liquid or gaseous state without having to digest/process the sample (avoiding adulteration of the sample). It also prevents losing efficiency due to the utilization of a cuvette/container.

Finally, this property allows to directly estimate the amount of Hg which might be sorbed by the container walls.

4.2.1 Energy Specific Element Selectivity

A huge advantage of using radioactive trackers is the energy specificity (figure 3). This allows us to study the behaviour of many toxic metals in the same sorption system simultaneously while studying the different elements/isotopes sorption, just by analysing their emission peaks individually (figure 3).

This characteristic warrants that any present non radioactive impurities will not interfere with the analysis and allows the study to be done in many kinds of solvents and/or matrices [3] since the γ emissions are in the high energy spectrum making the remaining elements "invisible" to the sorption study.

4.2.2 Tracking capability

Radioactive isotopes are widely used as tracers in many research fields, namely in medicine[25–27], *in vivo* experiments[28–30] and environmental issues[31–33].

This property enables the tracking of any path made by the radioactive isotopes which is quite convenient when studying the uptake of toxic metals. This tracking can give us information about the sorption capabilities of different parts of a given system.

For example, we can use radioactive trackers to feed a live animal/plant with a known amount of radioactive toxic metal and track the path made by the element of interest.

Using the experimental *setup* used in this manuscript (or any other analogous) we can also cut the plant/animal in pieces, label them and characterize the uptakes of Hg for each part of their anatomy (limited by the cutting resolution). This can give insight to biological sorption mechanisms since radioactive trackers are non intrusive and non destructive during all the uptake process. If one would want just a qualitative analysis we could also use gamma chambers to build a sorption map without having to destroy the sample.

4.3 Isotopes *à la carte*

The usage of radioactive trackers in the study Hg sorption can be extended to other toxic metals, as to any other element or compound, given an adequate radioactive isotope.

Facilities such as ISOLDE offer an astonishing *menu* of radioactive isotopes from where we can choose the tracker according to our experiment needs. The possibility of choosing many different isotopes also provides the ability (in some cases) to use hyperfine nuclear techniques (like Perturbed Angular Correlation, PAC, and Mössbauer Spectroscopy) to study the nanoscopic local properties and therefore understand the atomic/molecular mechanisms of coordination[34].

[3] The usage of different solvents and/or matrices can be an issue in fluorescence spectroscopy since they can interfere with the calibration curves

The Radioactive isotope half-life time will also influence the lower limit of detections, and therefore we can use a more accessible isotope with a longer half life as soon as the lower limit of detection remains adequate to our study.

5 Conclusions

We introduced an alternative method to characterize the uptake of Hg by sorption agents using Radioactive tracker spectroscopy, exploiting and combining well known fundamentals.

This manuscript serves as proof of concept, since it reproduces fairly well the results obtained in previous studies of Hg sorption by dithiocarbamate functionalized nanoparticles.

Radioactive Tracker Spectroscopy has conspicuous advantages when compared to typical fluorometry methods, being a direct, element specific type of uptake measurement with an unparalleled lower limit of detection of at least 10fg L^{-1}. Such remarkable sensitivity could be achieved using a fairly simple experimental setup and is mostly dependent of the quality of the HPGe detector and the isotope used. This sensitivity does not require any kind of processing or digestion of the sorption agent, being therefore a non destructive and non intrusive technique, which is also immune to the solvents and/or matrices of the sorbed material as well as to impurities (guaranteeing a clean and representative measurement of the uptake).

The tracking ability of the radioactive isotopes allows a path reconstruction for the sorption processes which enables new types of studies which were not possible using CVAFS, namely studies focusing in the behaviour of a given sorbent when exposed to external factors (such as temperature, pH, etc).

The usage of radioactive isotopes also enables the utilization of hyperfine techniques in parallel to the quantitative radioactive trackers uptake studies, unveiling local mesoscopic phenomena hence further enhancing our comprehension of sorption mechanisms of a given sorbent. We can as well bridge the Hg uptake studies to any element that we desire to study (namely other toxic and/or precious metals).

Lastly, this ultra-sensitive method is not intended to be used as an everyday substitute of CVAFS, but should be used instead either in situations where the above mentioned differentiating advantages are desirable or when the concentrations of Hg are too low to quantify with CVAFS. Hence using radioactive tracker spectroscopy to characterize and certify the sorption properties of FNP (or any other sorbent) from a given batch which in turn could be used as Hg concentrators and/or purifiers in waters where the concentrations of Hg are too low to quantify otherwise, is an immediate application for this approach.

6 Acknowledgements

The authors would like to thank the operation and technical ISOLDE teams and the Solid State Physics coordinator Dr. Juliana Schell. The authors would also like to thank Dr. James F. McNulty for his help during the writing reviewing of this manuscript.

This work has been supported by the Portuguese Foundation for Science and Technology (FCT) with projects CERN-FIS-NUC-0004-2015,PTDC/CTM-NAN/120668/2010, Pest-C/CTM/LA0011/2013, Pest-C/MAR/LA0017/2013, POCI-01-0145-FEDER-007679 - FCT Ref. UID /CTM /50011/2013, financed by national funds through the FCT/MEC, and, when appropriate, co-financed by FEDER under the PT2020 Partnership Agreement. FCT is also acknowledged for scholarship grants SFRH/BD/93336/2013 (C.O. Amorim), SFRH/BD/84743/2012 (A.S. Fenta), SFRH/BD/103828/2014

(D.S. Tavares), SFRH/BPD/99453/2014 (C.B. Lopes) and SFRH/BPD/82059/2011 (J. N. Gonçalves).

Other institutions are acknowledged: A.S. Fenta from support by the Scientific Research- Flanders (G.0983.15) and the KU Leuven BOF (CREA/14/013 and STRT/14/002) from Belgium. The German Federal Ministry of Education and Research (BMBF) through contract 05K13TSA and 05K16PGA is acknowledged for equipment used during experiments. The European Commission through the Horizon 2020 program (grant number 654002 ENSAR2) for support accessing the ISOLDE laboratory.

References

[1] F. Fu and Q. Wang, *J. Environ. Manage.*, 2011, **92**, 407–418.

[2] S. Babel and T. Kurniawan, *J. Hazard. Mater.*, 2003, **97**, 219–243.

[3] V. Gupta, P. Carrott, M. Ribeiro Carrott and Suhas, *Crit. Rev. Env. Sci. Tec.*, 2009, **39**, 783–842.

[4] G. Zhao, J. Li, X. Ren, C. Chen and X. Wang, *Environ. Sci. Technol.*, 2011, **45**, 10454–10462.

[5] R. D. Ambashta and M. Sillanpaa, *J. Hazard. Mater.*, 2010, **180**, 38–49.

[6] E. H. Borai, E. A. El-Sofany and T. N. Morcos, *Adsorption*, 2007, **13**, 95–104.

[7] I. Mohmood, C. B. Lopes, I. Lopes, I. Ahmad, A. C. Duarte and E. Pereira, *Environ. Sci. Pollut. Res.*, 2013, **20**, 1239–1260.

[8] D. S. Tavares, A. L. Daniel-da Silva, C. B. Lopes, N. J. O. Silva, V. S. Amaral, J. Rocha, E. Pereira and T. Trindade, *J. Mater. Chem. A*, 2013, **1**, 8134–8143.

[9] D. S. Tavares, C. B. Lopes, A. L. Daniel-da Silva, A. C. Duarte, T. Trindade and E. Pereira, *Chem. Eng. J.*, 2014, **254**, 559–570.

[10] R. Oliveira-Silva, J. P. da Costa, R. Vitorino and A. L. Daniel-da Silva, *J. Mater. Chem. B*, 2015, **3**, 238–249.

[11] P. I. Girginova, A. L. Daniel-da Silva, C. B. Lopes, P. Figueira, M. Otero, V. S. Amaral, E. Pereira and T. Trindade, *J. Colloid Interface Sci.*, 2010, **345**, 234–240.

[12] V. Mishin, V. Fedoseyev, H.-J. Kluge, V. Letokhov, H. Ravn, F. Scheerer, Y. Shirakabe, S. Sundell and O. Tengblad, *Nucl. Instrum. Methods Phys. Res., Sect. B*, 1993, **73**, 550–560.

[13] U. Köster, R. Catherall, V. Fedoseyev, S. Franchoo, U. Georg, M. Huyse, K. Kruglov, J. Lettry, V. Mishin and M. Oinonen, *Hyperfine Interact.*, 2000, **127**, 417–420.

[14] R. F. Mould, *A century of X-rays and radioactivity in medicine: with emphasis on photographic records of the early years*, CRC Press, 1993.

[15] S. B. Patel, *Nuclear physics: an introduction*, New Age International, 1991.

[16] D. Williams, *Methods in Experimental Physics*, 1976, **13**, 115 – 346.

[17] S. Halbach and R. Fichtner, *Toxicol. Methods*, 1993, **3**, 25–36.

[18] S. P. Mishra, V. K. Singh and D. Tiwari, *Radiochim. Acta*, 1996, **73**, 49–54.

[19] C. Pavel, K. Popa, N. Bilba, A. Cecal, D. Cozma and A. Pui, *J. Radioanal. Nucl. Chem.*, 2003, **258**, 243–248.

[20] A. A. A. Helal, *Radiochim. Acta*, 2006, **94**, 53–57.

[21] J. M. Haye, P. H. Santschi, K. A. Roberts and S. Ray, *Environ. Chem.*, 2006, **3**, 172–183.

[22] G. Hall and P. Pelchat, *Water Air Soil Poll.*, 1999, **111**, 287–295.

[23] E. Kopysc, K. Pyrzynska, S. Garbos and E. Bulska, *Anal. Sci.*, 2000, **16**, 1309–1312.

[24] T. Imasaka, H. Kadone, T. Ogawa and N. Ishibashi, *Anal. Chem.*, 1977, **49**, 667–668.

[25] M. Iyo, H. Namba, K. Fukushi, H. Shinotoh, S. Nagatsuka, T. Suhara, Y. Sudo, K. Suzuki and T. Irie, *Lancet*, 1997, **349**, 1805–1809.

[26] U. Veronesi, G. Paganelli, V. Galimberti, G. Viale, S. Zurrida, M. Bedoni, A. Costa, C. deCicco, J. Geraghty, A. Luini, V. Sacchini and P. Veronesi, *Lancet*, 1997, **349**, 1864–1867.

[27] D. Loebl, R. Craig, D. Culic, A. Ridolfo and F. Falk, Jand Schmid, *J. Am. Med. Assoc.*, 1977, **237**, 976–981.

[28] A. Zirlik, C. Maier, N. Gerdes, L. MacFarlane, J. Soosairajah, U. Bavendiek, I. Ahrens, S. Ernst, N. Bassler, A. Missiou, Z. Patko, M. Aikawa, U. Schoenbeck, C. Bode, P. Libby and K. Peter, *Circulation*, 2007, **115**, 1571–1580.

[29] D. Cagle, S. Kennel, S. Mirzadeh, J. Alford and L. Wilson, *Proc. Natl. Acad. Sci. U.S.A.*, 1999, **96**, 5182–5187.

[30] H. Sun, L. Mei, C. Song, X. Cui and P. Wang, *Biomaterials*, 2006, **27**, 1735–1740.

[31] J. Sanjurjo-Sanchez and C. Alves, *Environ. Chem. Lett.*, 2012, **10**, 131–143.

[32] C. Guimbaud, F. Arens, L. Gutzwiller, H. Gaggeler and M. Ammann, *Atmos. Chem. Phys.*, 2002, **2**, 249–257.

[33] F. Marcantonio, R. Anderson, M. Stute, N. Kumar, P. Schlosser and A. Mix, *Nature*, 1996, **383**, 705–707.

[34] J. G. Correia, K. Johnston and U. Wahl, *Radiochim. Acta*, 2012, **100**, 127–137.

Supplementary Information

Table S1 Sorption results for all the samples measured. Here we present the absolute number of Hg ions sorbed, its correspondent concentration in the solution used and the relative sorption value. Last line of the table shows an average of the standard error for each column.

Sample	N_{Hg}	C_{Hg} (ng/L)	ΔN_{Hg}	S (%)	NP	S_{Np} (%)
A_{2a}	3.5×10^{10}	9.7	6%	20 ± 2		
A_{2b}	3.9×10^{10}	10.8	6%	11 ± 1	A_2	14 ± 3
A_{2c}	4.8×10^{10}	13.1	6%	12 ± 2		
A_{4-a}	6.1×10^{10}	17	6%	74 ± 9		
A_{4-b}	1.4×10^{11}	38	7%	66 ± 9	A_{4-}	73 ± 7
A_{4-c}	2.2×10^{10}	6.2	6%	78 ± 10		
A_{4+a}	6.3×10^{10}	17	6%	66 ± 8		
A_{4+b}	7.3×10^{10}	20	6%	68 ± 9	A_{4+}	69 ± 6
A_{4+c}	1.18×10^{11}	32	7%	73 ± 10		
B_{2a}	7.8×10^{10}	22	6%	19 ± 2		
B_{2b}	6.2×10^{10}	17	6%	25 ± 3	B_2	25 ± 4
B_{2c}	3.7×10^{10}	10.1	6%	31 ± 4		
B_{4-a}	6.4×10^{10}	18	6%	49 ± 6	B_{4-}	50 ± 4
B_{4-b}	1.5×10^{10}	4.1	7%	50 ± 6		
B_{4+a}	3.9×10^{10}	10.6	6%	63 ± 8		
B_{4+b}	6.6×10^{10}	18	6%	74 ± 9	B_{4+}	69 ± 6
B_{4+c}	6.1×10^{10}	17	6%	69 ± 9		
	$\overline{\Delta N}_{Hg} = \overline{\Delta C}_{Hg} = 6\%$			$\overline{\Delta S} = 6\%$		$\overline{\Delta S}_{Np} = 5\%$